Time-to-Contact-Based Control Laws for Flare Trajectory Generation and Landing Point Tracking in Autorotation

Jonathan Rogers
Assistant Professor
Georgia Institute of Technology
Atlanta, Georgia
United States

Brian Eberle
Graduate Student
Georgia Institute of Technology
Atlanta, Georgia
United States

Michael Jump
Senior Lecturer
University of Liverpool
Liverpool,
United Kingdom

Neil Cameron
Research Associate
University of Liverpool
Liverpool,
United Kingdom

ABSTRACT

For many rotorcraft platforms, incorrect timing of the autorotation flare and deceleration maneuvers may result in significant aircraft damage and injury to the crew, or worse. There is a clear need for new pilot cueing and control augmentation technologies that lead to a higher probability of a successful autorotation landing. This paper describes a recent effort to develop two different Tau (time-to-contact)-based autorotation controllers that can be used to drive visual aids to help guide a pilot to apply the required control inputs to complete a safe autorotative landing. Such controllers may also be useful for fully autonomous autorotation landing for unmanned vehicles.

INTRODUCTION

Autorotation is a complex flight maneuver that requires several piloting tasks to be coordinated simultaneously in order to ensure a successful outcome. There is a continuing need to develop autorotation control laws that can serve in both automated roles for unmanned aerial vehicles, and as pilot assistance devices in difficult autorotation scenarios such as degraded visual environments, nighttime operations, or low-energy flight conditions. In such scenarios, pilot cueing may reduce workload, thereby allowing the pilot to focus on other important tasks which are difficult to automate such as selecting a suitable landing site. Likewise, for fully-autonomous or optionally-piloted vehicles, an automated autorotation landing system is likely to be required for certification in order to minimize risk in an emergency.

Numerous researchers have investigated autonomous autorotation control strategies both for use in autonomous aircraft and, to a more limited extent, as pilot training mechanisms or for in-flight pilot cueing. Initial work by Lee *et al*[1] used an optimal control approach to show that the height-velocity avoid region can be reduced significantly using automated autorotation control. Abbeel *et al*[2] and Dalamagkis *et al*[3] have studied machine learning strategies for autorotation control, with the former demonstrating successful autorotation of a model helicopter in flight experiments. More recently, Yomchinda *et al*[4] and Tierney and Langelaan[5] developed autorotation path planning and flare control laws, where the flare controller was derived through a direct optimal control approach. Several other authors, including Keller *et al*[6] and Bachelder *et al*[7], have developed autorotation control schemes designed as pilot-in-the-loop control augmentation systems or for pilot training. Additional ongoing work as part of Boeing's Helicopter Active Control Technology Program is addressing the problem of tactile feedback during steady-state autorotative descent using a neural network[8].

It is well-known that the most difficult aspect of autorotation to automate (besides selection of a landing site) is generation of a suitable, feasible flare trajectory[5]. This is a high-dimensional problem involving various state constraints and coupled nonlinear dynamics. The typical methodology employed in prior literature (i.e., Refs. 1, 4, 5, 7) is to discretize the control inputs in time over the flare trajectory and optimize them through an iterative process. Such an approach poses problems for certification due to convergence guarantees (if implemented online) or the ability to handle all possible landing scenarios (if implemented offline using a trajectory database). In an effort to develop real-time autorotation control laws which are compatible with certification requirements, the authors have developed a piecewise expert system controller that exhibits deterministic runtime and guaranteed convergence[9,10]. A key aspect of the control law developed in Refs. 9 and 10 is that the flare trajectory elapsed time is scaled based on the vehicle total kinetic energy, and the vehicle descent rate is then controlled to match this desired time-to-ground-contact. This approach allows the controller to derive feasible flare trajectories from a broad range of entry conditions. The use of time-to-contact in the closed-loop dynamics creates a bridge with a series of prior work on tau-based (or time-to-contact-based) flight guidance strategies developed by Jump and Padfield[11-13] for aircraft flare maneuvers. Using the previous controller as a starting point, recent efforts have focused on 1) formalizing and improving tau-based guidance strategies for autorotation,

Presented at the AHS International 74th Annual Forum & Technology Display, Phoenix, Arizona, USA, May 14-17, 2018.

and 2) investigating pilot cueing methodologies driven by time-to-contact controllers. The advantage of using tau-based guidance is illustrated in Ref. 19 where it was shown that tau-based strategies act as a natural inversion process, thus eliminating the vehicle dynamics from the guidance loop to achieve a given trajectory. An initial exploration of the latter objective was reported in Rogers *et al*[14], where it was shown that control inceptor cueing via a head-up display provided some benefit in autorotation maneuvers performed in degraded visual conditions. The work described here focuses on the former objective of tau-based formalization and does not address the topic of pilot cueing, which will be explored in future work.

Two coupled lines of effort are described: analyzing the time-to-contact control strategies used by pilots during autorotation and development of generalized flare control algorithms that use these identified strategies.

As an initial step, a series of piloted autorotation maneuvers was performed in the University of Liverpool flight simulator, and a common tau-guidance strategy (approximately) employed by all pilots was extracted from the simulated flight data. Only longitudinal axis control is considered in this paper as the pilot did not experience or report any handling qualities deficiencies in maintaining heading and bank angle during the autorotation. This common tau-guidance strategy was then used to create a tau-based flare control law for autorotation. Analysis of the pilot-in-the-loop autorotation simulations will be presented to identify the pilot control strategy and the corresponding tau strategies. It is hypothesized that to achieve a successful landing with a longitudinal-axis tau-based automatic controller, a control input strategy similar to that of the human pilot flying a successful maneuver manually should be generated. Mapping of the identified tau profile to the desired control inputs for each stage of the maneuver will be discussed in detail. Finally, further details of the controller implementation are presented and a comparison between the pilot-in-the-loop and the developed Automatic Autorotation Controller (AAC) results are discussed.

A second approach is to develop a controller from first principles which, in addition to flare trajectory generation and tracking, has the ability to land at or near a desired location on the ground. Previous work by Sunberg *et al*[9,10] and Rogers *et al*[14] did not address this requirement, focusing only on bringing the vehicle to a safe set of velocity and orientation conditions at ground impact. In this paper, the previous autorotation control law described in Ref. 9 is augmented using a tau-based forward deceleration profile. This deceleration profile uses a constant $\dot{\tau}$ trajectory, meaning that the derivative of the time-to-contact is held constant. During the flare maneuver, the time-to-ground contact is estimated using a kinematic approximation. This finite time horizon constraint is used to solve a two point boundary value problem (TPBVP) in terms of the forward position and velocity states. This TPBVP provides a time-varying velocity profile which can be tracked by an inner-loop controller. Because this TPBVP can be solved analytically, the solution time is deterministic (and can be computed quickly), and it can be updated at regular intervals throughout the flare to mitigate the effects of wind gusts or sudden changes in the desired landing location. This paper describes the formulation of this tau-based landing point trajectory generation algorithm, its integration into the previous autorotation control law from Ref. 9, and simulation results establishing its performance for an example aircraft.

TAU-BASED AUTOMATIC AUTOROTATION CONTROLLER

The first of the two methods aims to develop a Tau-based autorotation strategy for the longitudinal axis that can be displayed to a pilot during autorotation with the goal of improving touchdown performance and survivability. Touchdown performance was measured by comparing critical aircraft state touchdown parameters against desired and adequate touchdown metrics defined in Ref. 16 and listed in Table 1.

Table 1. Conditions for Successful and Marginal Landings

Parameter	Condition for successful landing	Condition for Marginal Landing
Pitch Angle θ	$<12^o$	$<20^o$
Forward Speed V_{des}	<30 knots	< 60 knots
Vertical Speed $\dot{Z}$	< 8 ft/s	<15 ft/s
Pitch Rate q	$-30^o/s < q < 20^o/s$	$-50^o/s < q < 40^o/s$

The process used to develop the system can be summarised in four key steps: 1) perform pilot-in-the-loop autorotation maneuvers; 2) assess pilot-in-the-loop simulation data to identify, where possible, Tau of height and Tau of longitudinal along-track distance strategies; 3) use these strategies to develop a Tau-based AAC and 4) present AAC controller output information (inceptor position or Tau information) to the pilot via a Head Up Display (HUD).

Steps 1-3 are described in detail in the subsequent sections The final step, to present the AAC controller output information (inceptor position or Tau information) to the pilot via a HUD and assess the impact on the pilot's ability to successfully land the helicopter simulation, will be reported at a later date.

Pilot-in-the-Loop Simulation

Pilot-in-the-loop autorotation maneuvers were performed using the University of Liverpool's HELIFLIGHT-R full-motion simulation facility[17] using a FLIGHTLAB-based generic rotorcraft simulation model. HELIFLIGHT-R,

illustrated in Figure 1, features a three channel 220 x 70 degree field of view visual system, a four-axis force feedback control loading system and an interchangeable crew station.

Figure 1. HELIFLIGHT-R simulator

The outside world imagery is generated using Presagis' Creator Pro software to produce either geo-specific or custom visual databases. Using Presagis' VEGA Prime software, the Liverpool Flight Science & Technology Group has generated its own run-time environment[17], LIVE (Liverpool Virtual Environment) which allows the simulator operator to change environmental effects such as daylight, cloud, rain and fog. A HUD can either be generated using an LCD screen with a beam splitter located above the instrument panel or projected directly onto the dome. The motion and visual cues, together with appropriate audio cues, provide an immersive environment for a pilot. Data from the flight models, e.g. aircraft accelerations, attitudes etc., together with pilot control inputs, can be monitored in real-time and recorded for post-flight data analysis.

Identification of Pilot Strategy

The final 300ft of the autorotation tasks flown by the test pilot are plotted in Figure 2 and the corresponding longitudinal axis touchdown performance is listed in Table 2. The x-axes of the charts are labelled as '*TimeToGo*' meaning that t = 0 is the time at main gear touchdown. Therefore, 'negative' time indicates the remaining task time

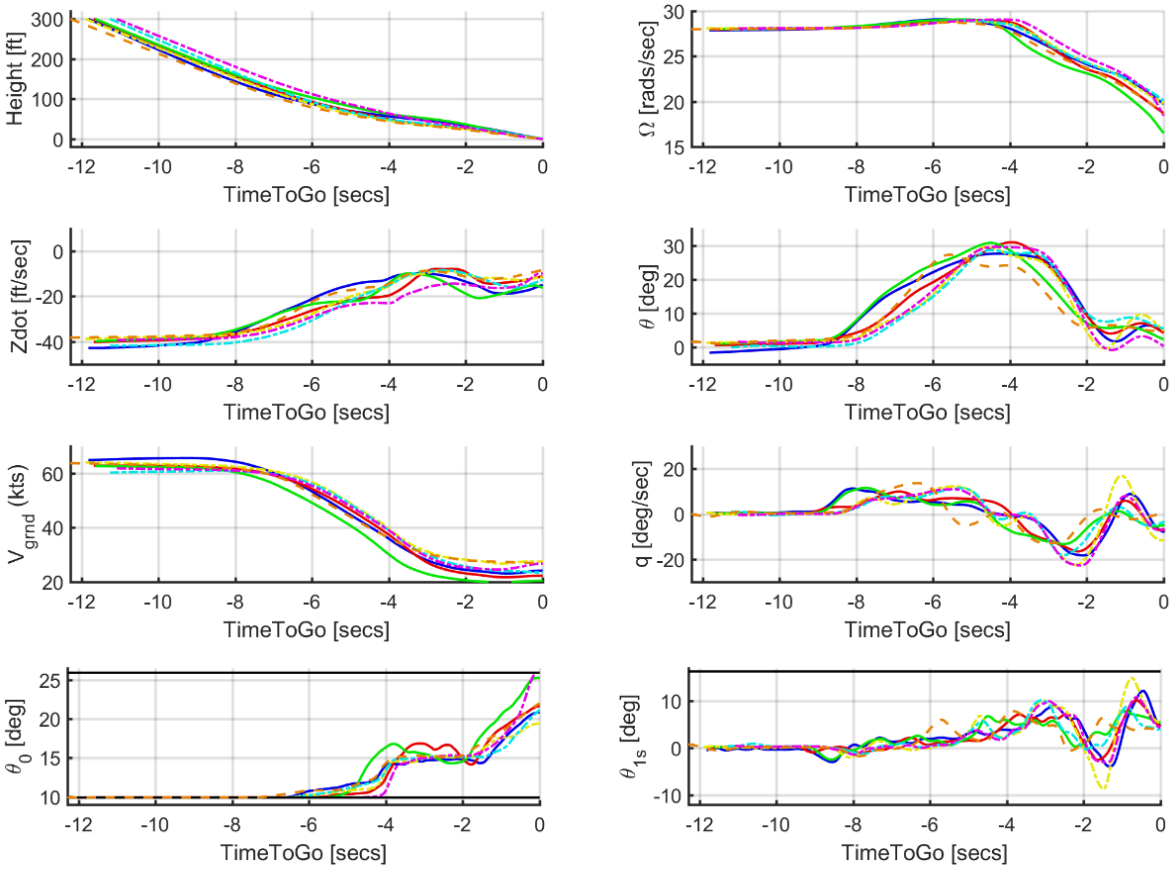

Figure 2. Flare phase Test Pilot-in-the-Loop Simulation of Autorotative landing

until touchdown.

After identifying the simulated engine failure, the pilot lowers the collective and adjusts the aircraft attitude to give a desired constant forward speed (V_{grnd}) and constant rate of descent (Z_{dot}). The start conditions are the same each time for the pilot-in-the-loop runs. However, the engine was failed manually by the simulator operator resulting in a different descent profile each time as the pilot was always aiming for the same landing point. At an altitude of approximately 200ft above the ground, the pilot initiates the flare by pulling back on the longitudinal stick. The flare consistently takes approximately 4 seconds to pitch the aircraft nose up to between 25 and 30 degrees. When the aircraft has reached task maximum pitch angle and the rotor speed has started to increase, the pilot applies a step input in collective (sometimes called a 'check'[18]) to maintain the rotor speed. This condition is held for a short period of time (approximately 2 seconds) to allow the descent rate and forward speed to reduce. The pilot next begins to level the aircraft pitch attitude (at an altitude of approximately 50ft). When pitch attitude has been significantly reduced (to less than 10 degrees) the pilot applies collective with a rate of change of approximately 5 degrees/second to further reduce the descent rate, cushioning the landing.

The longitudinal axis control strategy employed by the pilot to 'autorotate-to-land' the aircraft after an engine failure can be summarised as consisting of nominally four control inputs: 1) pull back on longitudinal cyclic stick to flare the aircraft (pitching up to approximately 30 degrees), reducing the descent rate and forward speed. This also causes the rotor speed to increase; 2) apply a step input in collective of approximately 30% to control the rotor speed; 3) push longitudinal cyclic stick forward to level the aircraft and 4) increase collective to cushion the landing.

Analysis of the touchdown performance against the requirements listed in Table 1 suggests that the pilot managed to reduce the longitudinal speed and level the aircraft attitude to well within the desired parameters each time. However, the descent speed at touchdown was only 'adequate' for the majority of test points.

Table 2. Test Pilot Touchdown Performance

	Vgrnd [ft/sec]	Vzi [ft/sec]	θ [deg]	q [deg/sec]
Desired	< 30	> -8	< 12	-30 -> 20
Adequate	< 60	> -15	< 20	-50 -> 40
	24.1789	-14.7460	4.4273	-8.3218
	22.2765	-11.0733	4.2735	-7.6430
	20.4819	-16.1115	2.3343	-5.3581
	27.5296	-11.4609	4.8095	-12.226
	23.3808	-12.624	5.5216	-3.9537
	26.8027	-9.7203	0.3794	-7.0977
	26.8263	-8.3205	4.8685	-0.1531

Tau Analysis of Piloting Strategy

The autorotation flare landing strategy is to be used to develop a controller based upon a τ_X and τ_H strategy where

$$\tau_X = \frac{X}{\dot{X}}, \quad \tau_H = \frac{H}{\dot{H}} \tag{1}$$

τ_H is the time to contact the ground in the vertical axis and τ_X is the time to contact a designated point a distance 'X' away at the current closure rate.

It is useful to consider how the longitudinal inceptor control strategy employed translates to the Tau domain and to identify the τ and $\dot{\tau}$ strategies adopted by the pilot in these simulation runs.

Figure 3 shows a constant $\dot{\tau}_H$ and $\dot{\tau}_X$ of approximately one during the steady state descent. This is entirely to be expected: a $\dot{\tau} = 1$ indicates a motion with constant velocity. The flare is initiated by pulling back on the longitudinal

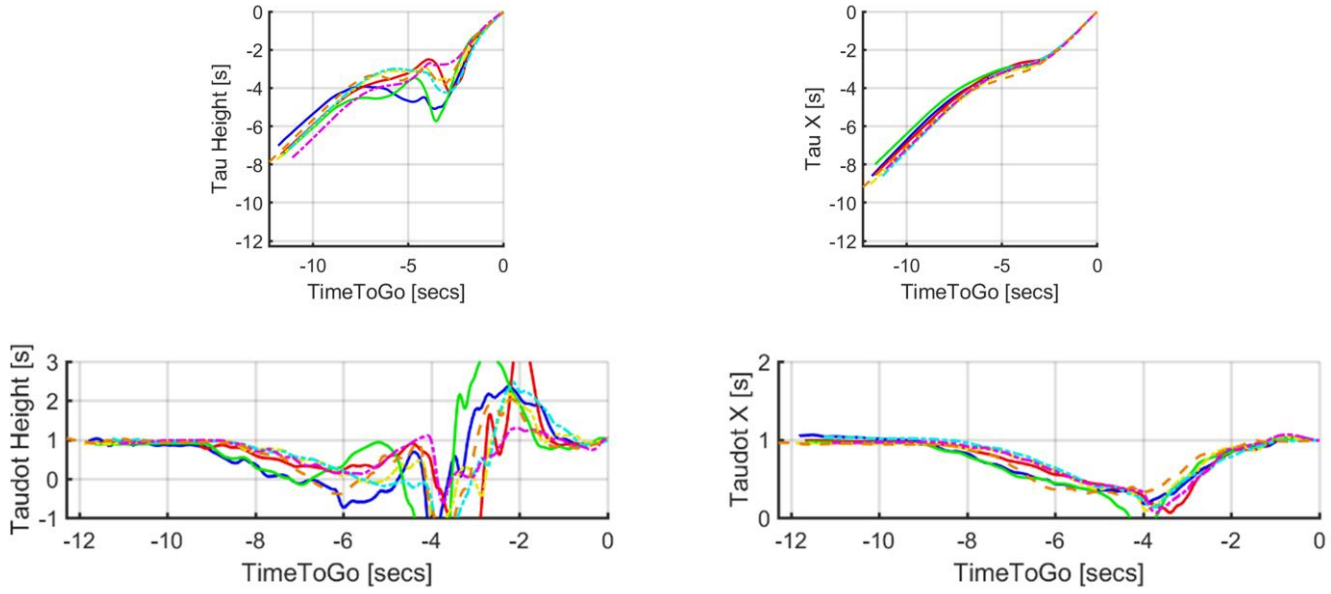

Figure 3. Tau Strategy for Flare phase by Test Pilot-in-the-Loop Simulation of Autorotative landing

cyclic, resulting in both $\dot{\tau}_H$ and $\dot{\tau}_X$ reducing. The rate of change of $\dot{\tau}_X$ profile is consistent over the series of runs where $\dot{\tau}_X$ reduces from one to a value close to zero with a constant rate of change between approximately 0.2 and 0.25/sec over a period of approximately 4-5 seconds. As the pilot levels the aircraft for landing, $\dot{\tau}_X$ returns to zero over a period of approximately 3 seconds. $\dot{\tau} = 0$ indicates a motion where the velocity (and hence distance to go) is reducing at an exponential rate.

Turning to $\dot{\tau}_H$, the rate of change of $\dot{\tau}_H$ is approximately 0.3 for the first 3 seconds after the flare is initiated. $\dot{\tau}_H$ varies significantly from run to run. A possible reason for this is that the collective check input is applied at different times or with different input magnitudes. Ideally during this phase, $\dot{\tau}_H$ should be held constant at a value close to zero, until the aircraft flight path begins to level off. At this point, $\dot{\tau}_H$ increases rapidly to two or more as when the longitudinal cyclic is pushed forward to level the aircraft. Consequently, the descent rate increases. Finally $\dot{\tau}_H$ is returned to one by increasing collective to cushion the landing.

Controller Development

The goal is to develop a Tau-based visual aid for the pilot to follow. However, if a proposed strategy will work for a pilot, then a Tau-based automatic controller should also be able to perform the task. Therefore this section details the development of a $\dot{\tau}$-based strategy for an automatic autorotation controller which will guide the aircraft to touchdown from a steady autorotative descent where $\dot{\tau}_H$ = 1 and $\dot{\tau}_X$ = 1.

From analysis of the pilot-in-the-loop data, one possible solution is to select $\dot{\tau}_H$ and $\dot{\tau}_X$ profiles which match the $\dot{\tau}_H$ and $\dot{\tau}_X$ pilot-in-the-loop test data as illustrated in Figure 4.

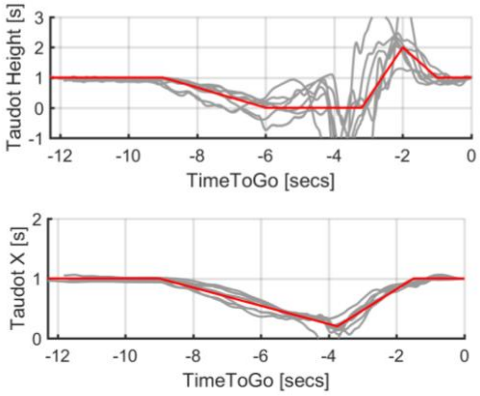

Figure 4. 'Ideal' $\dot{\tau}_H$ and $\dot{\tau}_X$ Strategies based upon Pilot-in-the-loop data

However, as previously discussed, the pilot consistently only achieved adequate performance in terms of descent rate at touchdown (-8 < $V_{zi,TD}$ > -15 ft/sec). This is partly due to $\dot{\tau}_H$ increasing to at least 2 when the aircraft pitch attitude is reduced in order to level the helicopter for landing. Therefore, the $\dot{\tau}_H$ strategy was adapted to that illustrated in Figure 5 in an attempt to try to improve the vertical speed at touchdown.

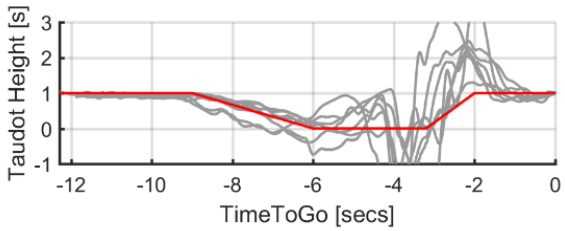

Figure 5. 'Implemented' $\dot{\tau}_H$ and $\dot{\tau}_X$ Strategies

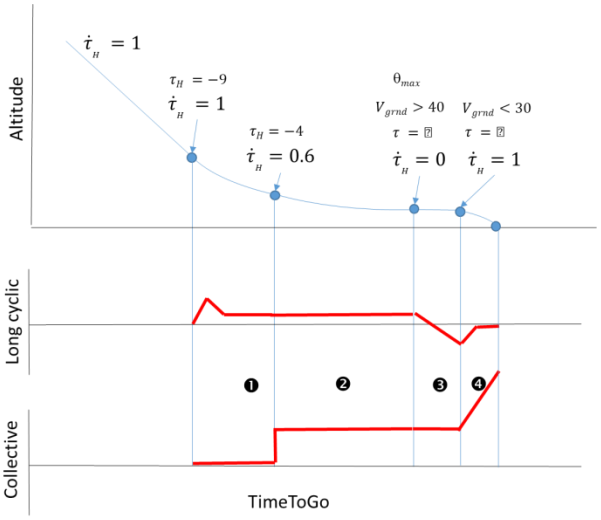

Figure 6. Control Implementation of Tau Strategy

Two control inputs, longitudinal cyclic and collective, are available for the pilot and AAC to control two $\dot{\tau}$ strategies. Therefore, the proposed Tau flare strategy is mapped back to the control input strategy as illustrated in Figure 6 to determine how and when the controls should be applied.

During the steady state descent phase, the pilot has trimmed the helicopter with a constant descent rate and forward speed ($\dot{\tau}_H$ and $\dot{\tau}_X$= 1). The pilot initiates the flare at approximately $\tau_X \approx$ -9 seconds by pulling back on the longitudinal cyclic stick which begins to reduce $\dot{\tau}_H$ and $\dot{\tau}_X$. It is hypothesised here that the pilot is flaring the aircraft primarily to reduce descent rate i.e. the pilot is controlling $\dot{\tau}_X$. When $\dot{\tau}_H$ has reduced, the pilot switches strategy. Collective pitch is applied to maintain rotor RPM and the desired descent rate, thus controlling $\dot{\tau}_H$, while the amount of pitch angle is selected to regulate the evolution of aircraft ground speed to be that needed at the selected landing point, i.e. $\dot{\tau}_X$. In this phase of flight, $\dot{\tau}_H$ and $\dot{\tau}_X$both tend towards a low value – 0.1 was therefore selected. This phase ends with the aircraft flying almost parallel to the ground below 50ft with a large nose-up pitch attitude. The pilot then prepares the aircraft for landing by levelling the aircraft. This will be triggered in the controller when several conditions have been met. First, when the ground speed has reduced below a threshold value

(40ft/sec) and when the vertical speed is greater than a threshold value, -7ft/sec. Finally, when the aircraft pitch attitude has reduced to an acceptable touchdown pitch angle, the pilot adds collective to further reduce the descent rate.

Controller Implementation

The controller has been developed as a PID controller based upon the desired $\dot{\tau}_{Hd}$ and $\dot{\tau}_{Xd}$ strategies determined from the current τ_X, τ_H, $\dot{\tau}_H$ and $\dot{\tau}_X$. Error signals $\dot{\tau}_{He}$ and $\dot{\tau}_{Xe}$ are then calculated for the current flight state and the outputs fed to the longitudinal cyclic channel and collective pitch channel. The controller is implemented in the FLIGHTLAB Control System Graphical Editor (CSGE) software and attached to the FLIGHTLAB simulation model.

Automatic Autonomous Controller Results

Results from the AAC-controlled aircraft descents as well as the pilot-in-the-loop time histories from which it was derived are shown in Figure 7. Touchdown performance of the AAC met all of the desired performance criteria, as shown in Table 3. Comparison of the AAC with test pilot results reveals that the control strategies are similar, including the collective 'check'. However, this happens earlier in AAC than in the pilot-in-the-loop runs as the pilot

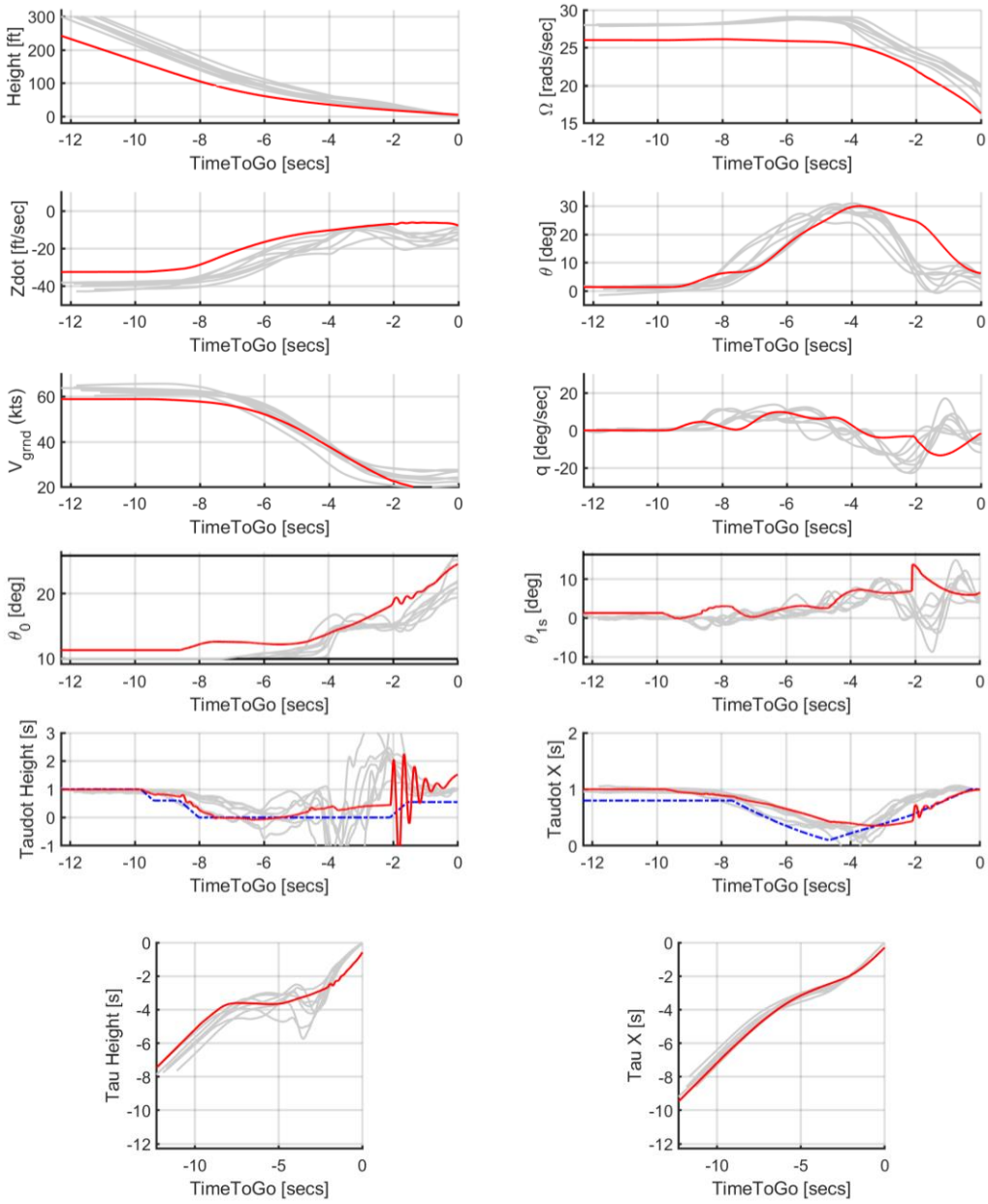

Figure 7. Comparison of Test Pilot and AAC Response.

is descending at a higher rate than the AAC, thus collective pitch in the AAC steady state is higher. The AAC controller tracks the commanded $\dot{\tau}_H$well for the first few seconds of the maneuver. Figure 7 illustrates that the return-to-level pitch attitude is initiated with approximately 2 seconds to touchdown. AAC pitch attitude remains high at this point in an effort to continue to reduce the aircraft forward speed and descent rate. Levelling the aircraft pitch attitude for touchdown requires a large longitudinal cyclic input (stick forward). For the manned case, the pilot increases collective pitch to maintain the descent rate within the desired parameter requirement. It is at this point the controller struggles to maintain the required $\dot{\tau}$ profile.

Table 3. Automatic autorotation Controller Touchdown Performance

	Vxi [ft/sec]	Vzi [ft/sec]	theta [deg]	q [deg/sec]
Desired	< 30	> -8	< 12	-30 -> 20
Adequate	< 60	> -15	< 20	-50 -> 40
	18.2	-7.7	6.2	-2.13

LANDING POINT TRACKING ALGORTIHM

Motivation

Any practical autorotation control law must provide the capability to manage the helicopter's vertical descent effectively to ground contact, but also ensure that the vehicle reaches a suitable (perhaps pilot-selected) landing location. The authors' previous autorotation control law documented in Ref. 9 was successful in the real-time generation of an autorotative flare trajectory that brings the vehicle to safe velocity and orientation conditions at ground impact from a wide range of autorotation entry states. Performance of this control law has been verified for fully-autonomous helicopters (Refs. 9 and 10) and when used to generate desired control inputs as part of a pilot cueing system (Ref. 14). However, the previous formulation of the control law did not incorporate any methodology to generate a forward speed deceleration profile so that a desired landing point is reached as the helicopter touches down. The ability to generate a forward speed deceleration trajectory that enables the helicopter to reach the target landing point at suitably slow vertical and forward speeds is known for the purposes of this paper as *landing point tracking*.

Landing point tracking is a necessary feature for an autorotation control methodology for fully-autonomous, optionally-piloted, or fully-piloted vehicles with cueing systems. A limited amount of work has been done in this area, particularly by Aponso and Bachelder (Ref. 7) and Tierney and Langelaan (Ref. 5). In both Ref. 5 and Ref. 7, the trajectory generation problem is formulated in an optimal control framework and solved offline with iterative methods. One potential problem with using such iterative optimization techniques is that trajectory planning must be done offline due to convergence and runtime considerations, and a large database must be generated and stored onboard in order to account for all helicopter weight configurations and wind conditions. Without a sufficiently large trajectory database, these planners may lack robustness to changes in vehicle parameters or outside disturbances. An alternative approach is to solve for a deceleration trajectory using a deterministic algorithm. Such a trajectory may not be optimal with respect to some cost function, but with proper formulation some constraint guarantees can be provided. Furthermore, given suitably short (deterministic) runtimes the planner can re-compute the deceleration trajectory during the flare as the situation changes, or as vehicle performance varies from that which is expected due to external perturbations or unknown system parameters.

This work documents the formulation of a real-time forward speed trajectory generator using a tau-based approach that provides a desired forward deceleration profile during the autorotation flare. Figure 8 shows a diagram of how this trajectory generation scheme can be integrated with the autorotation control law described in Ref. 9 and 10. During the flare phase of the autorotation, the collective channel is driven by the control law documented in Ref. 9 while the longitudinal cyclic is used to track the forward speed profile generated from the landing point tracking algorithm (described in the following section). This trajectory generator provides the controller the capability to track to a desired landing point during the flare phase of the autorotation. Note however that the trajectory generation scheme is limited to the flare phase only – a separate scheme would need to be used during steady state descent to ensure that the vehicle approaches the desired landing region effectively.

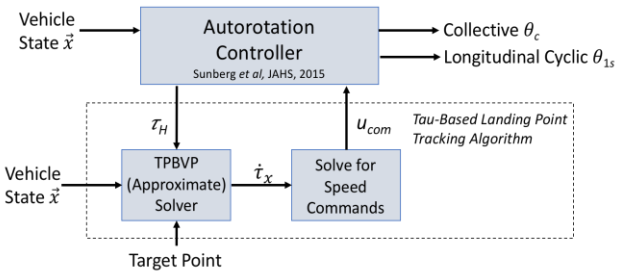

Figure 8. Landing Point Tracking Algorithm Integrated with Baseline Autorotation Control Law in Ref 9.

Mathematical Formulation

Define the lateral distance of the aircraft to the target landing point at any point during the autorotation flare as *x*. Following the tau-theory literature, the instantaneous time to contact of the helicopter with its targeted landing point is defined in Equation 1. The time derivative of this quantity is given by,

$$\dot{\tau}_x = 1 - \frac{x\ddot{x}}{\dot{x}^2} \tag{2}$$

Many studies of pilot behavior in the tau domain have shown that pilots tend to approach obstacles in a manner such that the derivative of the time-to-contact $\dot{\tau}$ remains a constant (Refs. 11-13,15), Using that assumption here, a constant k is defined according to,

$$1 - \dot{\tau}_x \equiv k = \frac{x\ddot{x}}{\dot{x}^2} \tag{3}$$

Note that k is a constant that shapes the relationship between x and its first and second time derivatives. Equation (3) is a second order ODE that can be rewritten as follows,

$$\dot{x} = v_x \qquad x(0) = x_i \tag{4}$$

$$\dot{v}_x = \frac{k v_x^2}{x} \qquad v_x(0) = v_{x,i} \tag{5}$$

where the initial conditions $x(0)$ and $v_x(0)$ are the state of the helicopter at the time that the trajectory is generated. This set of kinematic differential equations has a closed-form solution given in Ref. 19 as follows:

$$x(t) = x_i \left(1 - \frac{(k-1)v_{x,i}t}{x_i}\right)^{-\frac{1}{k-1}} \tag{6}$$

$$v_x(t) = v_{x,i} \left(1 - \frac{(k-1)v_{x,i}t}{x_i}\right)^{-1-\frac{1}{k-1}} \tag{7}$$

Equations (6) and (7) represent analytical solutions for the distance to the desired landing point and forward speed as functions of time. These nonlinear equations are parameterized by k, but cannot be solved for k in closed form.

The next step is to determine a value for k that results in the distance from the desired landing point being close to zero at the same time that the vertical descent is nearing completion. This ensures that the horizontal approach to the landing point and the vertical approach to the ground terminate at the same time. This can be viewed as a two point boundary value problem (TPBVP) where the time remaining in the horizontal direction is equal to that remaining in the vertical direction. To solve this problem, a prediction for the time-to-ground-contact T is needed. This value can be defined (in an instantaneous sense) as

$$T \equiv \frac{z_i}{v_{z,i}} \tag{8}$$

where z_i and $v_{z,i}$ are the altitude (AGL) and the vertical speed at the time of trajectory generation, respectively. While various techniques may be used to predict how much time the vehicle will remain in the air, simulation studies showed this instantaneous value to be an accurate predictor of the time to ground contact. Imposing this finite time horizon constraint and setting the distance from the desired landing point equal to a small threshold value yields,

$$x_i \left(1 - \frac{(k-1)v_i T}{x_i}\right)^{-\frac{1}{k-1}} = x_{TH} \approx 0 \tag{9}$$

Note that the small threshold value x_{TH}, which is a positive constant slightly larger than zero, must be used to avoid a singularity.

Equation (9) is now a 1D root-finding problem in which the only unknown value is k. This can be solved using a Newton-Raphson algorithm; however, because the range of acceptable k values is limited ($-1<k<1$), this range can be discretized into a mesh and each candidate solution for k can be evaluated in Equation (9). The k value that results in the right-hand-side closest to x_{TH} is taken as the approximately optimum value, k_o. The forward speed profile from Equation (7) then becomes,

$$v(t) = v_{x,i} \left(1 - \frac{(k_o - 1)v_{x,i}t}{x_i}\right)^{-1-\frac{1}{k_o-1}} \tag{10}$$

This forward speed profile is provided to the autorotation controller (shown as u_{com} in Figure 8) and is tracked by an inner-loop velocity tracking controller during the flare, landing, and touchdown phases of the maneuver (Ref. 9). Because the above solution avoids iterative optimization, the solution time for a flare trajectory is deterministic (and in practice quite fast given the simplicity of the equations). Values for k_o and T can be updated at regular intervals throughout the flare, enabling repeated trajectory updates which may act to mitigate the effects of wind gusts or sudden changes in the desired landing location.

Autonomous Simulation Results

The integrated autorotation controller and trajectory generation scheme was implemented in the helicopter flight dynamic simulation model documented in Ref. 9 and example simulation results were created for the SH-60B helicopter. Two example cases, shown in Figures 9 and 10, depict autorotation trajectories which target desired landing points near to the point of flare entry and far from flare entry, respectively. Both cases enter the flare at the same condition. The example shown in Figure 9 is targeting a landing point that is about 710ft downrange from flare entry, and the helicopter touches down 22ft beyond this point (a miss distance of less than one rotor radius). The forward and vertical speeds at touchdown are both within acceptable bounds for a safe landing. The pitch angle remains within acceptable bounds throughout the flare, but is somewhat high at touchdown. This could be moderated by adjusting the pitch angle limits during the landing and touchdown phases of the autorotation controller, although this development is left to future work. The last two subplots in Figure 9 show the desired forward speed and the optimum value of k computed by the trajectory generation algorithm (note that this data is on a different time scale than the

distance and pitch angle plots since the trajectory generator is only active after the flare phase has been initiated). In both examples, the *k* value is updated every two seconds to account for tracking error and changes in estimated time-to-ground contact. Although no wind is simulated here, these updates may also compensate for wind gusts. The *k* values and the shape of the desired speed curves do not vary significantly at each trajectory update, indicating that the preliminary estimate of time to ground contact is reasonably accurate and the tracking error is low.

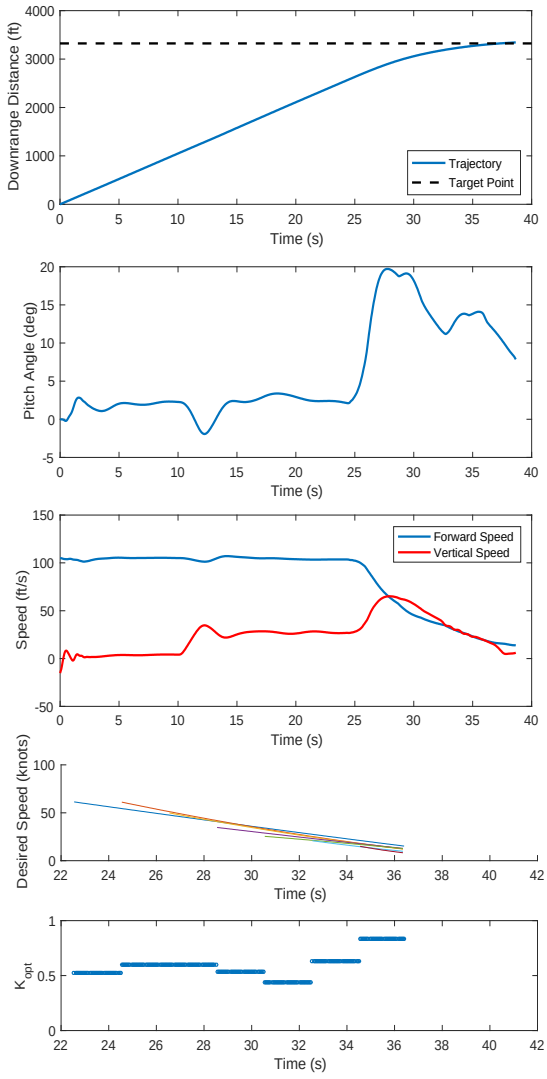

Figure 9. SH-60B Automated Autorotation with Landing Point Tracking, Example 1.

The example shown in Figure 10 targets a landing point 1,670ft downrange from flare entry and lands within 32ft of the target. Note that in this trajectory, the desired speed profiles are concave down (as opposed to the previous example) which induces the controller to maintain forward speed longer to stretch the glide. The helicopter pitch angle and vertical speed profiles are similar to the previous example except that the large pitch up maneuver in the flare is delayed due to the sustained higher forward speed. The penalty for stretching the glide to a farther target point is that the vehicle exhibits a high forward speed at touchdown. To slow the aircraft to a low forward speed late in the trajectory requires pitch angles that exceed the limits enforced by the autorotation control algorithm in close proximity to the ground, and thus only a mild speed reduction is achieved prior to touchdown. As in the previous example, note that the deceleration profile does not change significantly between updates, and the pitch angle at touchdown is again somewhat high as the aircraft attempts to decelerate just prior to landing.

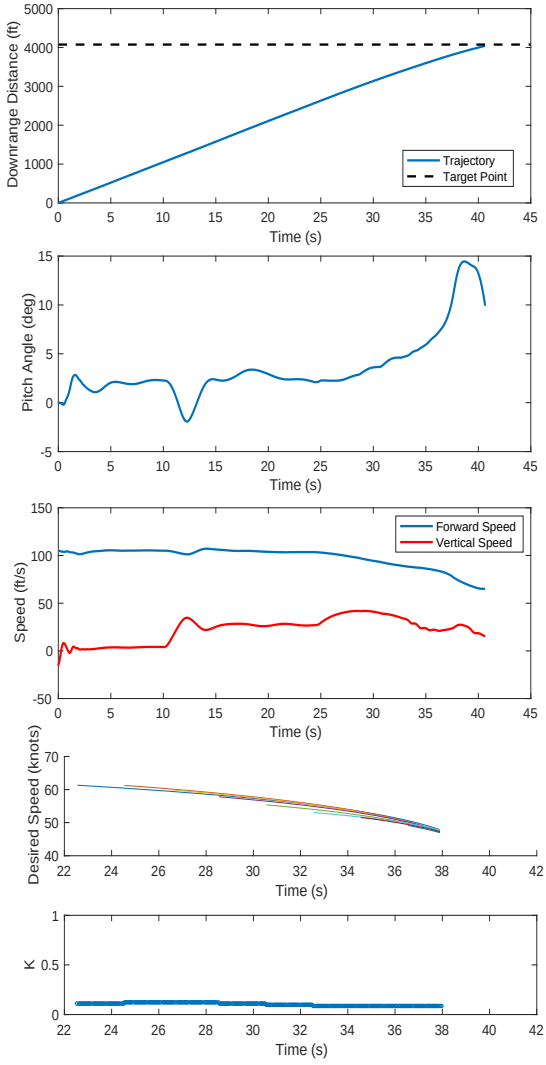

Figure 10. SH-60B Automated Autorotation with Landing Point Tracking, Example 2.

To better quantify the robustness of the algorithm and variations in performance when targeting landing points at different distances, a trade study was performed where the flare entry condition was held constant and the desired landing point was varied to 60 different target landing points. Figure 11 shows the flown trajectories from the trade

study overlaid on a single plot. It is clear from this plot that the trajectory generator can guide the helicopter to a wide range of desired landing points. Note in Figure 12 that the helicopter pitch angle profiles corresponding to trajectories targeting close-in landing points exhibit high pitch angles that could be considered unsafe or uncomfortable. On the other hand, trajectories targeting very far landing points require the helicopter to pitch down after flare initiation, which may also be inadvisable from a safety perspective. Examining Figure 13, which shows the flown velocity time histories for each case, it is clear that cases which pitch down after flare initiation are trying to accelerate to stretch the glide and often run out of rotor energy before being able to pitch up and slow down.

Figures 14-17 show some key trajectory metrics as a function of the target distance from flare entry. For each trajectory in the trade study, these metrics are computed and plotted in Figures 14-17. Figure 14 shows that landing distance error is maintained at a reasonably small value over a broad array of target landing points. It is also clear that at target distances which are too far from flare entry, the vehicle does not have sufficient energy to reach the target point and the aircraft lands short. Plots 15-17 depict key tradeoffs between maintaining landing point accuracy and ensuring safe flight conditions throughout flare and at touchdown. Figure 15 shows that the ground speed at touchdown increases as target distance increases, corroborating the trend shown in the example case above. Beyond a certain target point distance, the ground speed would likely be considered too fast for a safe landing. The maximum pitch angle observed during the flare, shown in Figure 16 as a function of the target point distance, is fairly constant except for very close and very far target points. The extreme pitch angles needed to land at points close to flare entry could disqualify target points that are nearer than a threshold distance from flare entry. These high pitch angles also result in increased inflow to the rotor disk, which causes an increase in rotor RPM as shown in Figure 17. A maximum rotor speed limit could also be enforced to provide a lower bound for a potential set of suitable landing points. Overall, the trajectory metrics shown in Figures 14-17 could be used to establish a bound on acceptable target point distances by enforcing limits on acceptable pitch angles in flare, touchdown speeds, and rotor speed, provided that such data can be generated or stored as the trajectory is computed. A practical method for enforcing these reachability criteria is the subject of ongoing work.

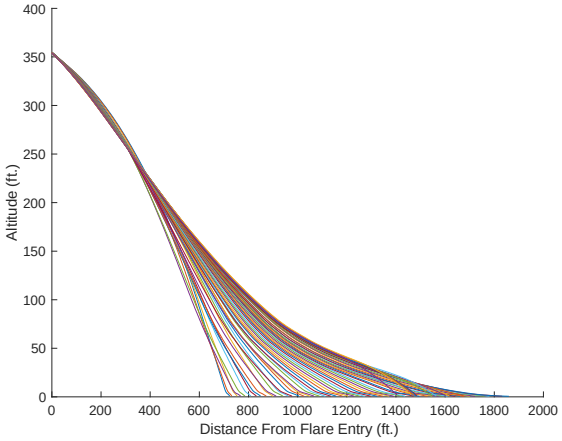

Figure 11. Altitude vs Distance From Flare Entry, Trade Study.

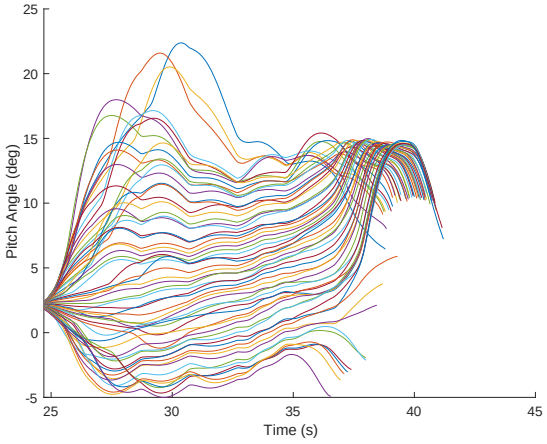

Figure 12. Pitch Angle vs Time, Trade Study.

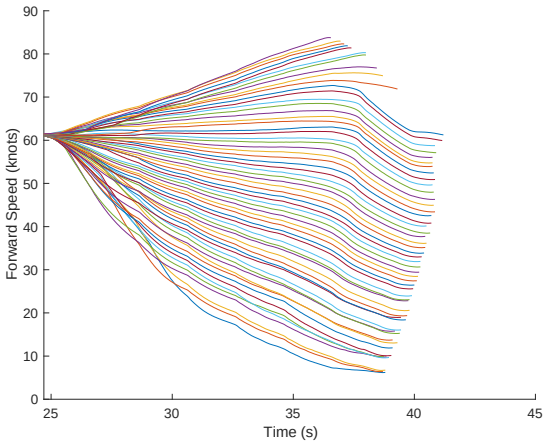

Figure 13. Forward Speed vs Time, Trade Study.

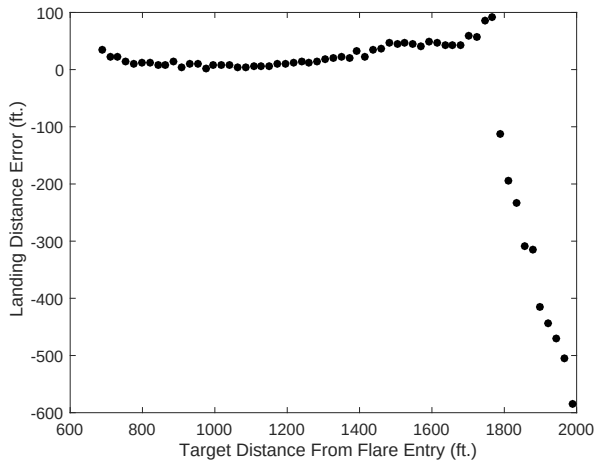

Figure 14. Landing Distance Error vs Target Distance, Trade Study.

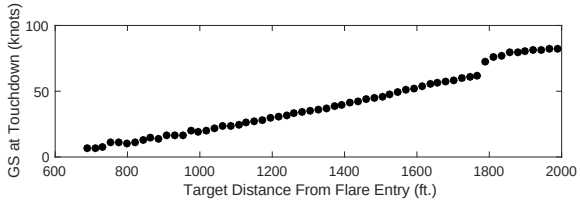

Figure 15. Groundspeed at Touchdown vs Target Distance, Trade Study.

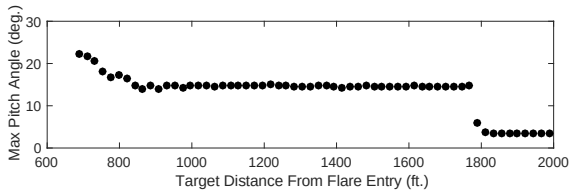

Figure 16. Maximum Pitch Angle vs Target Distance, Trade Study.

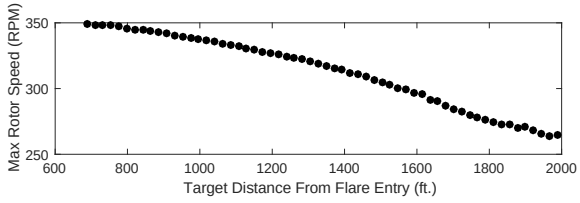

Figure 17. Maximum Rotor Speed vs Target Distance, Trade Study.

CONCLUSIONS AND FUTURE WORK

A Tau-based Automatic Autorotation Controller has been identified and implemented based upon analysis of pilot-in-the-loop simulation control strategy and the associated Tau profiles. Although results presented show that the aircraft lands successfully, meeting all of the desired touchdown criteria, further refinement is required. To transition this control law to manned systems, it will be employed within a cockpit display to drive display symbology to indicate desired collective pitch and longitudinal cyclic positions throughout the entire maneuver, from autorotation entry to touchdown.

In a related aspect of the work, a tau-based trajectory generation scheme has been formulated to produce a forward speed profile to be tracked during the autorotative flare for landing at a desired touchdown point. This trajectory generation scheme has the advantage of deterministic (and short) runtime allowing it to be implemented in an online and feedback fashion. Simulation studies show that the trajectory generator provides feasible forward speed profiles that enable the vehicle to land accurately at a range of desired locations. Future work will enforce state constraints during the trajectory generation process through use of a low-order model with deterministic runtime.

Author contact: Jonathan Rogers
(jonathan.rogers@me.gatech.edu)
Mike Jump (mjump1@liverpool.ac.uk)

ACKNOWLEDGMENTS

The research/investigation was sponsored by the Army Research Laboratory and was accomplished under Cooperative Agreement Number **W911NF-16-2-0027** and the U.S. Army/Navy/NASA Vertical Lift Research Center of Excellence with Mahendra Bhagwat serving as the Program Manager and Technical Agent, grant number **W911W6-11-2-0010** and **W911W6-17-2-0002.** The views and conclusions contained in this document are those of the authors and should not be interpreted as representing the official policies, either expressed or implied, of the Army Research Laboratory or the U.S. Government. The U.S. Government is authorized to reproduce and distribute reprints for Government purposes notwithstanding any copyright notation herein.

REFERENCES

[1]Lee, A. Y., Bryson, A. E., and Hindson, W. S., "Optimal Landing of a Helicopter in Autorotation," *Journal of Guidance, Control, and Dynamics*, Vol. 11, No. 1, 1988, pp. 7–12.

[2]Abbeel, P., Coates, A., Hunter, T., and Ng, A. Y., "Autonomous Autorotation of an RC Helicopter," *Experimental Robotics*, Vol. 54, 2009, pp. 385–394.

[3]Dalamagkidis, K., Valavanis, K. P., and Piegl, L. A., "Autonomous Autorotation of Unmanned Rotorcraft using Nonlinear Model Predictive Control," *Journal of Intelligent and Robotic Systems*, Vol. 57, (1–4), September 2009, pp. 351–369.

[4]Yomchinda, T., Horn, J. F., and Langelaan, J.W., "Flight Path Planning for Descent-Phase Helicopter Autorotation," AIAA Guidance, Navigation, and Control Conference, Portland, OR, August 8–11, 2011, pp. 1–24.

[5]Tierney, S. and Langelaan, J., "Autorotation path planning using backwards reachable set and optimal control," American Helicopter Society Forum, 2010.

[6]Keller, J. D., McKillip, Jr., R. M., Horn, J. F., and Yomchinda, T., "Active Flight Control and Applique Inceptor Concepts for Autorotation Performance Enhancement," AHS International 67th Annual Forum Proceedings, Virginia Beach, VA, May 3–5, 2011.

[7]Bachelder, E. N., Lee, D.-C., and Aponso, B. L., "Autorotation Flight Control System," U.S. Patent 7976310 B2, 2011.

[8]Nicholas, J., and Miller, D., "Method, system, and computer program product for tactile cueing flight control," U.S. Patent 6735500 B2, 2004.

[9]Sunberg, Z., Miller, N., and Rogers, J., "A Real Time Expert Control System for Helicopter Autorotation," *Journal of the American Helicopter Society*, Vol. 60, 2015, pp. 1-15.

[10]Sunberg, Z., Miller, N., and Rogers, J., "A Real Time Expert Control System for Helicopter Autorotation," 70th Forum of the AHS, Montreal, Canada, May 20-22, 2014.

[11]Jump, M., and Padfield, G. D., "Investigation of the Flare Maneuver Using Optical Tau," *Journal of Guidance, Control, and Dynamics*, published online Sept. 2006; Vol. 29, No. 5, pp. 1189-1200. doi: 10.2514/1.20012

[12]Jump, M., and Padfield, G. D., "Progress in the Development of Guidance Strategies For the Landing Flare Maneuver Using Tau-based Parameters," *Aircraft Engineering and Aerospace Technology*, published online 2006; Vol. 78, No. 1, pp. 4-12. doi:10.1108/17488840610639618

[13]Padfield G.D., Lu, L., and Jump, M., "Tau Guidance in Boundary-Avoidance Tracking - New Perspectives on Pilot-Induced Oscillations," *Journal of Guidance, Control, and Dynamics*, published online Jan. 2012; Vol. 35, No. 1, pp. 80-92. doi:10.2514/1.54065

[14]Lu, L., Jump, M., & Padfield, G. D. (2017). Development of a Generic Time-to-Contact Pilot Guidance Model. Journal of Guidance, Control, and Dynamics, 1-12. doi:10.2514/1.G003135

[15]Rogers, J., Strickland, L., Repola, C., Jump, M., Cameron, N., Fell, T., "Handling Qualities Assessment of a Pilot Cueing System for Autorotation Maneuvers," 73rd Forum of the AHS, Ft. Worth, TX, May 9-11, 2017.

[16]Padfield G.D., "The Tau of Flight Control," *The Aeronautical Journal*, Vol. 115, No. 1171, September 2011, pp. 521-556.

[17]White, M.D., Perfect, P., Padfield, G.D., Gubbels, A.W. & Berryman, A.C., Acceptance testing and commissioning of a flight simulator for rotorcraft simulation fidelity research, Proceedings of the IMechE, Part G: Journal of Aerospace Engineering, 2012, **226**, (4), pp 638-686. DOI: https://doi.org/10.1177/0954410012439816

[18]Coyle, S, 'Cyclic and Collective", , LuLu.com, 2009 ISBN: 978-0557090662

[19]D. Lee, "A Theory of Visual Control of Braking Based on Information About Time-to-Collision," *Perception*, Vol. 5, 1976, pp. 437-459.

[20]Lu, L., Jump, M., & Padfield, G. D. "Development of a Generic Time-to-Contact Pilot Guidance Model," *Journal of Guidance, Control, and Dynamics*, Vol. 41, 2017, pp. 1-12. *doi:10.2514/1.G003135*